BCR/ABL oncogenic kinase promotes unfaithful repair of the reactive oxygen species–dependent DNA double-strand breaks

Michal O. Nowicki, Rafal Falinski, Mateusz Koptyra, Artur Slupianek, Tomasz Stoklosa, Ewa Gloc, Margaret Nieborowska-Skorska, Janusz Blasiak, and Tomasz Skorski

The oncogenic BCR/ABL tyrosine kinase induces constitutive DNA damage in Philadelphia chromosome (Ph)–positive leukemia cells. We find that BCR/ABL-induced reactive oxygen species (ROSs) cause chronic oxidative DNA damage resulting in double-strand breaks (DSBs) in S and G_2/M cell cycle phases. These lesions are repaired by BCR/ABL-stimulated homologous recombination repair (HRR) and nonhomologous end-joining (NHEJ) mechanisms. A high mutation rate is detected in HRR products in BCR/ABL-positive cells, but not in the normal counterparts. In addition, large deletions are found in NHEJ products exclusively in BCR/ABL cells. We propose that the following series of events may contribute to genomic instability of Ph-positive leukemias: BCR/ABL → ROSs → oxidative DNA damage → DSBs in proliferating cells → unfaithful HRR and NHEJ repair. (Blood. 2004;104:3746-3753)

Introduction

The *bcr/abl* chimeric gene is derived from relocation of part of the *c-abl* gene from chromosome 9 to part of the *bcr* gene locus on chromosome 22 (t(9;22), Philadelphia chromosome [Ph]) and is present in most patients with chronic myelogenous leukemia (CML) and in a cohort of patients with acute lymphocytic leukemia (ALL).[1,2] BCR/ABL exhibits 2 complementary roles in cancer: it stimulates signaling pathways that render leukemia cells independent of their environment, and it modulates the response to DNA damage causing drug resistance.[3,4] In contrast to normal cells, BCR/ABL-positive cells seem to be better equipped to survive genotoxic damage because of their enhanced ability to repair DNA lesions, prolonged activation of the G_2/M checkpoint to provide more time for repair, and inhibited proapoptotic mechanisms.[5] Clinical observations and experimental findings have shown that BCR/ABL also stimulates genomic instability, leading to mutations and chromosomal abnormalities.[6-12] The accumulation of genetic errors is believed to be responsible for the transition from a relatively benign CML chronic phase (CML-CP) to the aggressive blast crisis phase (CML-BC). Aberrations in pathways regulating the DNA damage response in BCR/ABL-positive leukemia cells may contribute to this phenomenon.

DNA damage can directly result from genotoxic treatment or may simply occur as a consequence of genome duplication infidelity or of genotoxic effects of compounds such as reactive oxygen species (ROSs). ROSs are generated as a normal byproduct of normal oxidative metabolism in eukaryotic cells, and they can cause damage to all molecules, including DNA.[13] Single-strand oxidative DNA damage, including species such as 8-oxoguanine (8-oxoG), has been documented for many years.[14] If not repaired, the damage can induce a number of deleterious effects, including mutations[15] and double-strand breaks (DSBs),[16] leading to elevated cancer risk.[17]

BCR/ABL kinase–stimulated ROSs[18] may exert chronic genotoxic stress, causing DNA damage in leukemia cells. Given that mechanisms necessary for the repair of DNA lesions might be altered by BCR/ABL,[10,19-22] the probability of accumulating DNA errors seems to be much higher in BCR/ABL-positive cells than in nontransformed cells because more DNA damage occurs, and, though overall repair capability is enhanced, the fidelity of repair mechanisms is compromised. A mutator phenotype may be essential for tumor cells to grow in various organs under diverse conditions and to resist antitumor treatments.

This work shows that BCR/ABL elevates the level of ROSs, resulting in numerous DSBs during genome duplication and division (S and G_2/M phases). Unfortunately, the oncogene promotes unfaithful mechanisms of DSB repair. We hypothesize that elevated levels of DSBs, combined with unfaithful repair mechanisms, may contribute to genomic instability and malignant progression of Ph-positive leukemias.

Materials and methods

Cells

The murine growth factor–dependent myeloid cell line 32Dcl3 and BCR/ABL- or BCR/ABL[K1172R]-expressing clones[20] have been maintained in the presence of pretested optimal concentrations of interleukin-3 (IL-3) required to maintain their continuous proliferation. Bone marrow

From the Center for Biotechnology, College of Science and Technology, Temple University, Philadelphia, PA; and the Department of Molecular Genetics, University of Lodz, Poland.

Submitted May 25, 2004; accepted July 27, 2004. Prepublished online as *Blood* First Edition Paper August 10, 2004; DOI 10.1182/blood-2004-05-1941.

Supported by grants from the National Institutes of Health and the American Cancer Society (T.S.), the Oncology Research Faculty Development Program from the National Cancer Institute (T.S.), and the Leukemia Research Foundation (A.S.). T.S. is a Scholar of the Leukemia and Lymphoma Society.

An Inside *Blood* analysis of this article appears in the front of this issue.

Reprints: Tomasz Skorski, Molecular Carcinogenesis Section, Center for Biotechnology, College of Science and Technology, Temple University, Bio-Life Sciences Bldg, Rm 419, 1900 N 12th St, Philadelphia, PA 19122; e-mail: tskorski@temple.edu.

The publication costs of this article were defrayed in part by page charge payment. Therefore, and solely to indicate this fact, this article is hereby marked "advertisement" in accordance with 18 U.S.C. section 1734.

mononuclear cells from C57Bl/6 mice (mBMCs) (The Jackson Laboratory, Bar Harbor, ME) were infected with breakpoint-cluster region/Abelson leukemia–internal ribosomal entry site–green fluorescence protein (BCR/ABL-IRES-GFP) or IRES-GFP retroviral particles, as described.[20] GFP-positive cells obtained after sorting were cultured for 72 hours in the presence of pretested concentrations of IL-3 and were used for experiments. Bone marrow cells from patients with CML (2 with CML chronic phase and 2 with CML blast crisis) and healthy donors (hBMCs), described before,[23] were obtained after informed consent. Mononuclear cells were cultured for 72 hours in the presence of pretested recombinant human IL-3 and stem cell factor (SCF), and $CD34^+$ cells were isolated.[24] Draa-40[25] and BCR/ABL-Draa-40 cells were cultured in Dulbecco modified Eagle medium (DMEM) supplemented with 10% fetal bovine serum (FBS).

Inhibitors

Cells were treated with the following compounds: 2 μM imatinib mesylate (STI571; Novartis Pharma AG, Basel, Switzerland), 0.2 μM antioxidant pyrrolidine dithiocarbamate (PDTC), 100 μM nitrone spin traps *N-tert*-butyl-*a*-phenylnitrone (PBN) and 5,5-dimethyl-1-pyrroline-*N*-oxide (DMPO), and 2 μM wortmannin and 5 mM caffeine (Sigma-Aldrich, St Louis, MO). Imatinib mesylate, PDTC, PBN, and DMPO were added for 48 hours; wortmannin and caffeine were added for 3 hours.

Comet assay

Comet assay was performed under alkaline conditions, as described,[26] with modifications.[27] Comet tail moment was analyzed in 50 images randomly selected from each sample, in duplicate experiments (total, 100 images/sample); it positively correlates with the level of DNA breakage and alkali-labile sites.[28] The value of tail moment in particular samples was taken as an index of DNA damage. Because our measurement system was not calibrated, tail moment was presented in arbitrary units. Results represent mean ± SEM. Data were analyzed using the Statistica (StatSoft, Tulsa, OK) statistical package. For enzyme treatment, cells were drained in agarose and covered with an enzyme buffer (control) or with the enzyme (1 μg/mL endonuclease III [EndoIII] or formamidopyrimidine-DNA glycosylase [(Fpg]) in buffer, incubated for 30 minutes at 37°C, as described,[29] and the comet tail moment was analyzed as described here. Results obtained with buffer only were subtracted from these, obtained with an enzyme (enzyme treatment usually increased the detection of DNA damage by approximately 2-fold).

DNA fragmentation analysis

Genomic DNA was isolated from 3 to 5×10^6 cells using the DNeasy Tissue Kit (Qiagen, Valencia, CA), and 2 to 3 μg was run (30 V for 15 minutes, followed by 70 V for few hours) in 2.5% agarose gel containing ethidium bromide and was then photographed.

ROS assay

Levels of intracellular ROSs were analyzed in cells growing in the presence of IL-3 using the redox-sensitive fluorochrome 2′,7′-dichlorofluorescin-diacetate.[18]

HRR assay

Draa-40 cells[25] and BCR/ABL–Draa-40 cells[20] have integrated 1 or 2 copies of the modified gene for GFP (*DR-GFP,* which contains an I-*Sce*I site) as a recombination reporter and a fragment of the GFP gene (which contains a *Bcg*I site) as a donor for homologous repair. A homologous recombination repair (HRR) event restores functional GFP expression (*Bcg*I positive), which is readily detected by flow cytometry.

NHEJ assay

Nonhomologous end joining (NHEJ) was measured in cell-free extracts as described,[30] with modifications.[31] Briefly, 10^7 cells were washed 3 times with ice-cold phosphate-buffered saline (PBS), and cytoplasm lysis was performed on ice for 10 minutes in hypotonic buffer A (10 mM HEPES [*N*-2-hydroxyethylpiperazine-*N*′-2-ethanesulfonic acid], 1.5 mM $MgCl_2$, 10 mM KCl, pH 7.5) and in proteinase inhibitors (2 μg/mL aprotinin, 2 μg/mL leupeptin, 0.5 mM phenylmethylsulfonyl fluoride [PMSF], 0.5 mM dithiothreitol [DTT], 25 mM NaF, 0.2 mM $NaVO_3$). Cell pellets were spun down for 3 minutes in 6000*g* at 4°C, and cytoplasmic lysis was repeated. A pellet containing nuclei was resuspended in buffer B (20 mM HEPES, 25% glycerol, 500 mM NaCl, 1.5 mM $MgCl_2$, 0.2 mM EDTA [ethyleneglycotetraacetic acid], pH 7.5) and in proteinase inhibitors as in buffer A, and it was rapidly frozen and thawed 3 times (liquid nitrogen/37°C). Whole mixture was centrifuged at 30 000*g* for 30 minutes at 2°C. Supernatant was dialyzed overnight against buffer C (25 mM Tris-HCl, pH 7.5, 1 mM EDTA, 10% glycerol) containing proteinase inhibitors as in buffer A. Aliquots of nuclear protein samples were stored in −70°C. NHEJ reactions were performed under the following conditions. A mixture containing 10 μg nuclear lysate, 1 mM adenosine triphosphate (ATP), 0.25 mM dNTPs, 25 mM Tris-acetate, pH 7.5, 100 mM potassium acetate, 10 mM magnesium acetate, and 1 mM DTT was preincubated in 37°C for 5 minutes. The substrate—200 ng linear plasmid pBluescript KS+ (digested *Xho*I + *Xba*I to generate noncompatible 5′ overhangs)—was added to the reaction mix and incubated for 1 hour at 37°C. Samples were then incubated with 1 μg proteinase K in 65°C for 30 minutes. Products of NHEJ reaction were resolved in 0.5% agarose gel containing 0.5 μg/mL ethidium bromide, scanned with Adobe Photoshop, and analyzed by ImageQuant TL (Amersham Bioscience, Piscataway, NJ).

Measurements of the DNA repair frequency and fidelity

Draa-40 parental and BCR/ABL-Draa-40 cells were transfected with I-*Sce*I expression plasmid, and the frequency and fidelity of DSB repair was examined as described by Pierce et al,[32] with modifications. Briefly, 3 days after I-*Sce*I transfection, a fragment of the DR-GFP cassette containing a putative DSB repair site was amplified by polymerase chain reaction (PCR) using DR-GFP cassette-specific primers: forward (A), CAGCCATTGCCTTTTATGGT; reverse (B), GCCTGAAGAACGAGATCAGC. Products were cloned into the TA cloning kit (Invitrogen, Carlsbad, CA) plasmid and were transformed into the One Shot TOP10. Bacterial colonies containing *Bcg*I site (HRR product) or I-*Sce*I site (replication product) or not containing either site (NHEJ product) were identified by Southern dot blotting using the *Bcg*I- and I-*Sce*I specific probes GGTGGCATCGCCCTCGCC and GGTATTACCCTGTTATCCCTAGCCGGA, respectively (hybridization conditions allowed detection of a sequence containing one mismatched base). The presence of the NHEJ product in the *Bcg*I/I-*Sce*I double-negative colonies was confirmed by PCR. Repair products were amplified from bacteria by PCR using the forward (C) AGGGCGGGGTTCGGCTTCTGG and reverse (D) CCTTCGGGCATGGCGGACTTGA primers to amplify the HRR products[32] and commercially available T3 and T7 primers to amplify the NHEJ products (primers spanning larger fragments of DR-GFP cassette were used here to reduce the chance of omitting more extensive deletions), and sequenced. HRR mutation frequency was calculated as total number of mutated nucleotides/total number of sequenced nucleotides. Identical mutations detected in *Bcg*I-positive sequences and in I-*Sce*I–positive sequences (20 sequences/group analyzed) were subtracted from the calculation to exclude replication errors. An average gain/loss of the bases in the double-negative *Bcg*I-/I-*Sce*I-NHEJ sequences was determined by dividing the sum of acquired/deleted bases by the number of sequences. Twenty repair products (HRR and NHEJ)/experimental group were analyzed.

Immunofluorescence

Nuclear localization of the indicated proteins was detected by immunofluorescence, as previously described.[10] Briefly, cytospins from unsynchronized cells were fixed in PBS with 0.06% Triton X-100 and 4% formaldehyde, washed in PBS and 0.06% Triton X-100, and blocked in washing buffer supplemented with 1% bovine serum albumin (BSA). To perform cell cycle–specific analysis, cells were washed with PBS, spun down, gradually resuspended in ice-cold fixing buffer (PBS with 0.06% Triton X-100, 4% formaldehyde, and 0.04% glutaraldehyde), and incubated on ice for 30 minutes. Fixed cells were washed twice with PBS, resuspended in 1 mL PBS with 100 μg RNase DNase-free (Roche, Mannheim, Germany), and

incubated at room temperature for 15 minutes. DNA was stained with propidium iodide as described.[5] G_0/G_1, S, and G_2/M cell populations were isolated by fluorescence-activated cell sorter (FACS) and cytospun. FACS was used to confirm the cell cycle purity of sorted cell populations. Cells were stained with first antibodies against γ-H2AX (Upstate Biotechnology, Lake Placid, NY) and RAD51 (PC130; Oncogene Research Products, Cambridge, MA) or Ku70 (AHP318, Serotec, Raleigh, NC). Secondary antibodies conjugated with Alexa Fluor 488 or Alexa Fluor 568 were applied (Molecular Probes, Eugene, OR). Negative controls were performed without primary antibodies. DNA was counterstained with DAPI (4′,6′diamedino-2-phenylindole). Specific staining was visualized using an inverted Olympus IX70 fluorescence microscope equipped with 100 × UPlan Apo lens (numeric aperture 1.35), and a Cooke Sensicam QE camera (The Cooke Company, Auburn Hills, MI). At least 50 individual cells were analyzed per experimental group, as described.[10] Images were acquired with Slidebook 3.0 (Intelligent Imaging Innovations, Denver, CO). All graphic adjustments were performed using Adobe Photoshop.

Linker-ligation PCR assay

Genomic DNA was purified using the DNeasy Tissue Kit (Qiagen). The protocol for linker-ligation PCR (LL-PCR) to detect broken-ended, double-stranded DNA, described by Schlissel et al,[33] was followed with modifications. Briefly, the 2 oligomers BW-1 (GCGGTGACCCGGGAGATCTGAATTC) and BW-2 (GAATTCAGATC) were annealed to form a linker and were stored frozen. Purified DNA (2 μg) was incubated with Klenow polymerase and ligated to the linker. Ligated DNA (200 ng) was used in a 50 μL PCR assay containing 3 pmol linker reverse primer (BW-1) and DR-GFP cassette-specific forward primer (AGGGCGGGGTTCGGCTTCTGG) or Na^+/K^+ ATPase-specific forward primer (GCATTGACTTGGGCACTGAC) and 2 U Taq polymerase. After 2 rounds of PCR (2 × 20 cycles), the products were detected by Southern blot analysis using α-dCTP–labeled DR-GFP probe (*Nar*I-*Hpa*I fragment of the *DR-GFP* gene) and γ-ATP labeled Na^+/K^+ ATPase–specific probe (GGCCTACGAGCAAGCTGAG oligomer), respectively.

Results

BCR/ABL elevates the levels of ROSs to induce DSBs

Comet assay indicated that the presence of BCR/ABL kinase increased the level of DNA damage (strand breaks and abasic sites) on average by approximately 2.5-fold. Inhibition of the kinase by 48-hour incubation with 2 μM imatinib mesylate[34] or ROSs by 48-hour incubation with the antioxidants (0.2 μM PDTC,[18] 100 μM PBN, and 100 μM DMPO[35]) reduced the damage to the level detected in parental cells (Figure 1A). Imatinib mesylate and the antioxidants inhibited intracellular ROSs (data not shown). In agreement, gel electrophoresis also detected chromosomal fragmentation of the genomic DNA in BCR/ABL cells, but not in parental cells or in BCR/ABL cells treated with imatinib mesylate or PDTC (Figure 1B), implicating DNA breaks occurring specifically in a BCR/ABL kinase–dependent, ROS-mediated manner. To directly detect the oxidative damage of DNA, we used 2 enzymes, EndoIII and Fpg, which convert oxidative lesions into gaps detectable by the comet assay. Adding EndoIII or Fpg to the comet reaction significantly increased the DNA damage in BCR/ABL cells relative to parental cells; again, oxidative DNA damage levels were abrogated by the inhibition of BCR/ABL kinase with imatinib mesylate and the reduction of ROSs by PDTC (Figure 1C).

To characterize the DNA breaks in BCR/ABL cells, histone γ-H2AX was used to quantitate DSBs and to spatially localize them within the nuclei of cells. γ-H2AX seems to result from a specific ATM/ATR-dependent phosphorylation of histone H2AX on serine 139 in chromosome regions encompassing megabase lengths of DNA adjacent to DSBs.[36-38] Approximately 60% of the exponentially growing BCR/ABL-32Dcl3 cells contained γ-H2AX foci compared with 20% of parental cells (Figure 2A). To confirm that this effect occurs also in primary cells, mBMCs were infected with BCR/ABL retroviral particles. Approximately 61% of BCR/ABL-positive growth factor–independent mBMCs displayed γ-H2AX foci, in contrast to only 27% of normal counterparts (Table 1). Moreover, CML primary cell populations contained more γ-H2AX foci–positive cells than normal cells (17% and 2%, respectively; 4 patients with CML and 3 healthy donors were analyzed). The generally lower levels of γ-H2AX foci–positive healthy human cells, compared with their murine counterparts, may depend on the differences in basal oxidative damage levels; the former cells contain approximately 10 times fewer oxidized lesions than the latter ones.[39]

The γ-H2AX foci were formed in response to DNA damage–dependent activation of ATM/ATR kinases because wortmannin and caffeine (inhibitors of these kinases[40]) dramatically reduced the number of foci (Table 1). Inhibiting BCR/ABL kinase by imatinib mesylate and blocking of ROSs by PDTC diminished the percentage of γ-H2AX–positive BCR/ABL cells (Table 1). This result implicates the BCR/ABL kinase–dependent, ROS-mediated mechanism leading to the elevated levels of leukemia cells bearing DSBs. In addition to the increased percentage of BCR/ABL-positive cells displaying γ-H2AX foci, these cells contained at least 2-times more foci per cell than their nontransformed counterparts (Figure 2A). The percentages of γ-H2AX-positive cells containing 10 or less, and more than 10 foci per nucleus were 3% and 97%, respectively, in BCR/ABL-32Dcl3 cells, in contrast to 75% and 25%, respectively, in parental 32Dcl3 cells.

To determine whether γ-H2AX foci were associated with a particular cell cycle phase, exponentially growing 32Dcl3 parental cells and BCR/ABL-32Dcl3 cells were sorted on the G_0/G_1, S, and

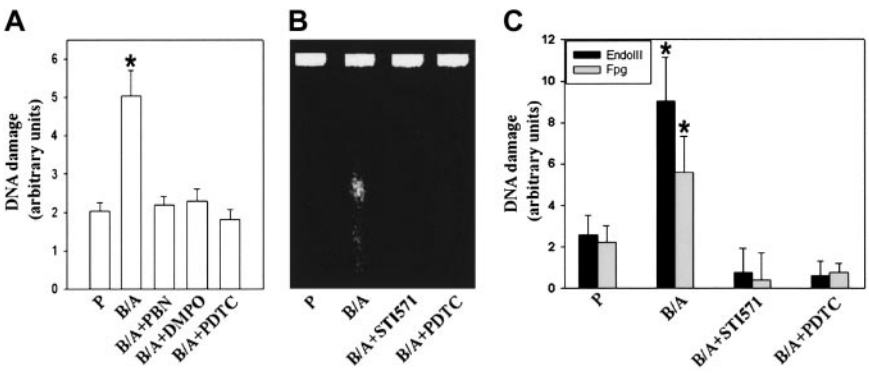

Figure 1. BCR/ABL-induced ROSs cause oxidative DNA damage. 32Dcl3 parental (P) and BCR/ABL-32Dcl3 cells (B/A) were cultured in the presence of IL-3; 2 μM imatinib mesylate, 0.2 μM PDTC, 100 μM DMPO, and 100 μM PBN were added for 48 hours when indicated. (A) Spontaneous DNA damage was detected by the comet assay. (B) Native genomic DNA was run through an ethidium-stained 2.5% agarose gel. (C) Oxidative damage to DNA was probed by EndoIII endonuclease and Fgp glycosylase and was detected by the comet assay. Bars represent the enzyme-dependent increase of DNA damage over that detected in the undigested samples. The error bars represent standard deviation. *$P < .05$ compared with other experimental groups.

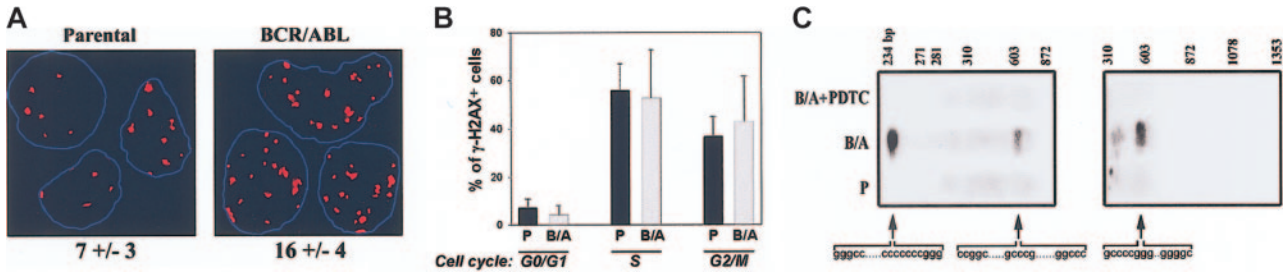

Figure 2. BCR/ABL-induced ROS causes DSBs in S and G_2/M cell cycle phases. (A) Representative 32Dcl3 parental and BCR/ABL-32Dcl3 nuclei containing γ-H2AX foci. Only the foci colocalizing with DAPI are shown; nuclei borders are marked in blue. Numbers below show the mean number ± SD of foci per nucleus. (B) γ-H2AX foci were detected in 32Dcl3 parental (P) and BCR/ABL-32Dcl3 (B/A) cells isolated in G_0/G_1, S, and G_2/M cell cycle phases. Results show mean percentages plus or minus standard deviation of cell cycle distribution of the cells containing γ-H2AX foci. (C) DSBs (depicted by arrows) in the DR-GFP sequence (left panel) and Na^+/K^+ ATPase sequence (right panel) were detected by LL-PCR followed by Southern blotting in BCR/ABL-positive cells (B/A), but not in parental (P) and PDTC-treated BCR/ABL-positive cells (B/A-PDTC). The G/C-rich stretches near the predicted DSB sites are listed.

G_2/M populations according to DNA content. Analysis of cell cycle distribution of γ-H2AX–positive cells revealed that most cells were in S and G_2/M phase but not in G_0/G_1 phase; BCR/ABL did not change their percentage distribution (Figure 2B).

LL-PCR was used to detect DSBs to confirm the results obtained with the use of γ-H2AX foci as a marker of DSBs. We found 2 hotspots for DSBs in the *DR-GFP* gene in BCR/ABL-Draa-40 cells. These DSBs were not detectable in parental cells or in BCR/ABL cells if ROSs were inhibited by PDTC (Figure 2C, left panel). In addition, DSBs in the α1 subunit of the *Na^+/K^+ ATPase* gene were detected by LL-PCR in BCR/ABL-32Dcl3 cells but not in parental 32Dcl3 cells (Figure 2C, right panel). Again, PDTC inhibition of ROSs prevented detection of these DSBs in BCR/ABL cells. Combined analysis of the approximate lengths of LL-PCR products, position of the forward primers, and *DR-GFP* or *Na^+/K^+ ATPase* gene sequences revealed multiple G/C-rich sequences at the predicted DSB hotspots (Figure 2C).

As expected, increased levels of ROS-dependent DSBs in the *DR-GFP* gene in BCR/ABL cells were associated with increased levels of spontaneous HRR, as measured by the detection of GFP-positive cells after 8 weeks of cell culture. HRR rate (estimated using Luria-Delbruck fluctuation analysis, with modifications[41]) was 30×10^{-4} and 3.5×10^{-4} for BCR/ABL-Draa-40 cells and Draa-40 parental cells, respectively. BCR/ABL-Draa-40 cells incubated in the presence of PDTC displayed a reduced HRR rate, 11×10^{-4}, compared with untreated BCR/ABL-Draa-40 cells.

Table 1. γ-H2AX nuclear foci detection by immunofluorescence

Cells	γ-H2AX–positive	*t* test, *P* value less than
P	20 ± 6	—
B/A	60 ± 13	10^{-10} v P
P + Wt/Caff	5 ± 1	10^{-4} v P
B/A + Wt/Caff	19 ± 2	10^{-7} v B/A
B/A + STI571	30 ± 6	10^{-7} v B/A
B/A + PDTC	29 ± 5	10^{-6} v B/A
mBMC	27 ± 8	—
mBMC-B/A	61 ± 14	10^{-6} v mBMC
hBMC	2 ± 1	—
CML	17 ± 2	10^{-4} v hBMC

Numbers indicate the mean percentages plus or minus standard deviation of cells with γ-H2AX foci (at least 5 foci/cell). Statistical significance (*P*) of the results versus other experimental groups is shown.

P indicates 32Dc13 parental cells; B/A, BCR/ABL–positive counterparts; Wt/Caff, cells treated with wortmannin + caffeine; B/A + STI571, B/A cells treated with imatinib mesylate; B/A + PDTC, B/A cells treated with PTDC; mBMC, normal murine bone marrow cells; mBMC-B/A, BCR/ABL–transformed cells; hBMC, human BMC from healthy donors; CML, human BMC from patients with CML; —, not applicable; and v, versus.

BCR/ABL stimulates HRR and NHEJ to facilitate the repair of ROS-dependent DSBs

Because most cells containing DSBs are in the S and G_2/M cell cycle phases, DSBs could be repaired by either of the 2 competing machineries, HRR or NHEJ.[42-44] The efficiency of HRR and NHEJ in BCR/ABL-positive and -negative cells was examined using the specific tests.

A copy of the DR-GFP cassette containing inactivated *GFP* gene, resulting from the introduction of the unique I-*Sce*I restriction site containing 2 stop codons, and a truncated version of the gene were integrated into the genome of Draa-40 cells.[25] DSB is generated in the *GFP* gene upon transient transfection with I-*Sce*I expression plasmid, which could be repaired by HRR using the truncated fragment of the gene as a template, thus producing a functional gene and, hence, GFP-positive cells. Draa-40 cells containing the DR-GFP cassette were transfected with expression plasmids containing BCR/ABL wild-type, BCR/ABL[K1172R] kinase-inactive mutant ($BCR/ABL_{[kin-]}$), or empty plasmid; the expression of BCR/ABL proteins was confirmed by Western blot analysis (not shown). These cells were then transfected with I-*Sce*I expression plasmid (and the β-galactosidase plasmid to control the transfection efficiency), and HRR frequency was measured by scoring the percentage of GFP-positive cells. The presence of BCR/ABL active kinase, but not the kinase-dead mutant, caused an approximately 4-fold increase in the percentage of GFP-positive cells, implicating activation of the HRR mechanism (Figure 3A).

pBluescript plasmid linearized by *Xho*I + *Xba*I digestion creating noncomplementary 5‘ overhangs was used as the substrate to assess the activity of NHEJ, which generates the products containing multimers of plasmid.[30,45] The substrate was added to cell lysates from 32Dcl3 parental, BCR/ABL wild-type, and BCR/ABL[K1172R] kinase-inactive ($BCR/ABL_{[kin-]}$) cells, and NHEJ products were analyzed by agarose gel electrophoresis. BCR/ABL kinase activity was responsible for more than a 5-fold increase of NHEJ activity; inactivation of the kinase by point mutation (K1172R) reduced NHEJ by 3-fold (Figure 3B).

HRR and NHEJ reaction sites in the nuclei could be potentially visualized by double-immunofluorescence detecting colocalization of γ-H2AX foci with RAD51 or Ku70, respectively.[46] As shown in Figure 3C, approximately 50% of DSBs marked as γ-H2AX foci colocalized with RAD51 in parental and BCR/ABL-positive 32Dcl3 cells; similarly, approximately 50% of the γ-H2AX foci colocalized with Ku70. This suggests that HRR and NHEJ are equally important for the repair of ROS-mediated DSBs in BCR/ABL cells.

Parental cells treated for 48 hours with 100 μM buthionine-sulfoximine (BSO), which inhibits γ-glutamyl-cysteine synthetase,

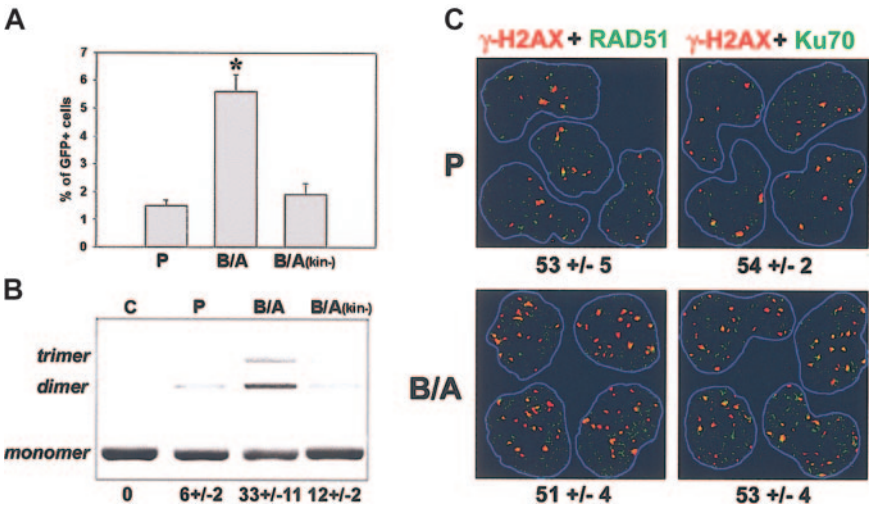

Figure 3. BCR/ABL-induced DSBs are repaired by HRR and NHEJ. (A) HRR-dependent restoration of a functional GFP protein (GFP-positive cells) after I-*Sce*I–mediated induction of a DSB in Draa-40 parental (P), BCR/ABL-Draa-40 (B/A), and BCR/ABL$_{(kin-)}$-Draa-40 (B/A(kin−)) cells (bars represent mean plus or minus standard deviation; *$P < .05$ compared with other experimental groups). (B) NHEJ-mediated end ligation of the *Xho*I + *Xba*I–digested plasmid substrate (monomers) by the lysis buffer (C) or cell lysates from 32Dcl3 parental (P), BCR/ABL-32Dcl3 (B/A), and BCR/ABL$_{(kin-)}$-32Dcl3 (B/A$_{(kin-)}$) cells, generating multiplasmid products (dimers, trimers). Mean ± SD percentages of end-joined substrate are shown below ($P < .05$, B/A compared with BCR/ABL$_{(kin-)}$; $P < .01$ B/A compared with P). (C) Colocalization (yellow) of γ-H2AX (red) with Rad51 or Ku70 (both green) in the representative 32Dcl3 parental (P) and BCR/ABL-32Dcl3 (B/A) nuclei, whose borders are outlined in blue. Numbers indicate mean ± SD percentages of colocalization.

thus increasing ROSs by depleting glutathione pools,[47] displayed an enhancement of ROSs (data not shown) and an increased percentage (56 ± 11) of γ-H2AX–positive cells (compare with group P in Table 1). However, the elevation of ROS-mediated DSBs in parental cells was not associated with enhanced HRR (1.36% ± 0.3% of GFP-positive cells) and NHEJ (5.8% ± 1.8% of repair) compared with the untreated cells (Figure 3A-B, group P). Finally, approximately 10% to 20% of BSO-treated cells have been displaying an apoptotic signature (subdiploid amount of DNA) after 72 hours of incubation. These effects were reversed by the antioxidant PDTC (data not shown), implicating ROSs dependence.

BCR/ABL promotes mutagenic repair of DSBs

Parental and BCR/ABL-Draa-40 cells were transfected with I-*Sce*I expression plasmid to inflict a DSB in the reporter DR-GFP cassette. The primers spanning a fragment of the DR-GFP cassette containing the DSB site were used 72 hours later to amplify the repair products by PCR, which were then analyzed by Southern assay and sequenced to determine the frequency and fidelity of a repair mechanism (Figure 4A). Sequences with restored *Bcg*I restriction site were considered HRR product, those without *Bcg*I and I-*Sce*I sites were identified as NHEJ products, and those with

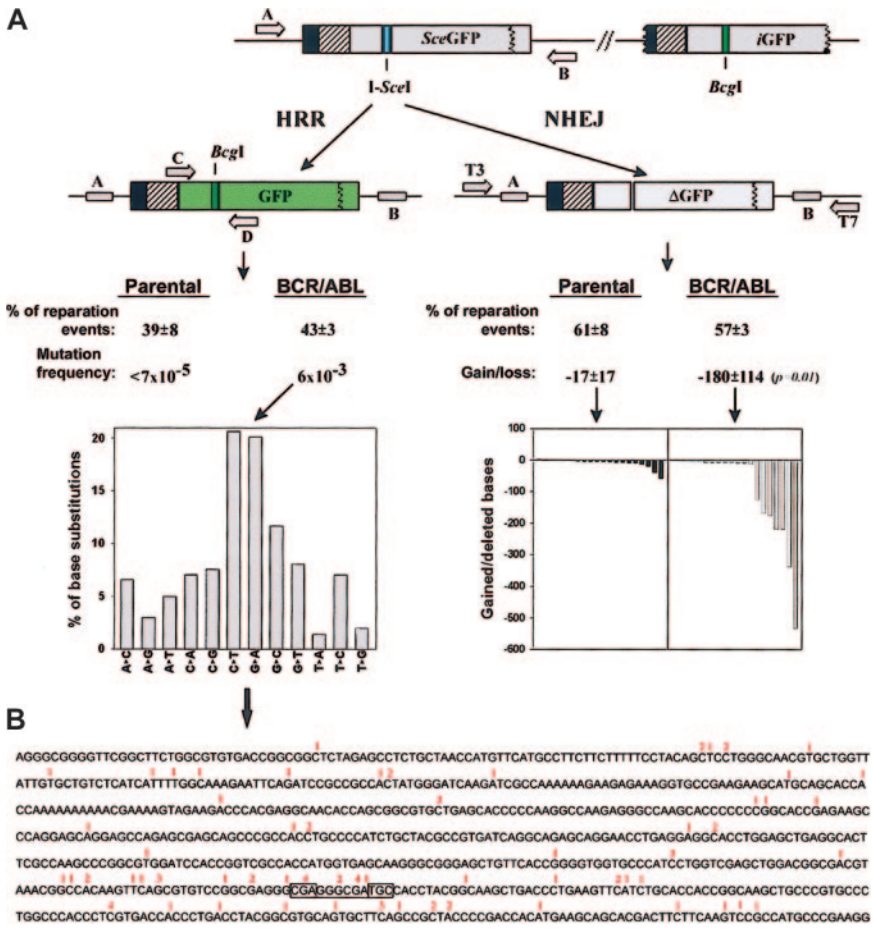

Figure 4. BCR/ABL promotes unfaithful repair of DSBs. Parental and BCR/ABL-Draa-40 cells were transfected with I-*Sce*I expression plasmid to induce a DSB in the reporter DR-GFP cassette. (A) The scheme illustrates the consequences of I-*Sce*I–induced DSB in DR-GFP. HRR restores *Bcg*I restriction site (left branch), and NHEJ results in the loss of both I-*Sce*I and *Bcg*I sites (right branch). Repair products were amplified 72 hours later by PCR using primers A and B, cloned, and expressed in the competent bacteria. HRR (*Bcg*I-positive) and NHEJ (*Bcg*I-negative/I-*Sce*I-negative) products were identified by Southern analysis (200 bacterial clones/group analyzed), amplified by PCR using primers C and D, or T3 and T7, respectively, and sequenced (20 sequences/group analyzed) to determine the repair mechanism (percentage of reparation events) and its fidelity (mutation frequency for HRR, and gain/loss of DNA base pairs for NHEJ). The mutation phenotype in the 725-bp HRR products in BCR/ABL cells is shown in the bottom left diagram; gain/loss of DNA in the individual NHEJ products in parental and BCR/ABL cells is shown in the bottom right diagram. (B) Individual mutations in the HRR products in BCR/ABL cells are shown (red numbers indicate the number of mutations detected at the particular base). *Bcg*I restriction site sequence is boxed.

preserved I-*Sce*I site are considered the replication products (DSB and repair did not occur).

Combined PCR–Southern blot analysis revealed that HRR and NHEJ consist of approximately 40% and 60% of DSB repair products, respectively, and that BCR/ABL does not significantly change this proportion (Figure 4A, % of repair events), though it enhances HRR and NHEJ activity (Figure 3A-B). HRR products obtained from parental cells were repaired faithfully (no mutations found), whereas the products from BCR/ABL-positive cells contained mutations (overall mutation rate, 6×10^{-3}) (Figure 4A, HRR branch). Analysis of the mutations revealed that almost 55% of mutations involved G/C → A/T transitions (40.4%) and G/C → T/A transversions (14.3%), 2 of the most common mutations resulting from oxidative DNA damage.[15] These mutations do not cluster near the DSB site (Figure 4B). Typical deletions or additions (range, +3 to −59 bp) were detected in NHEJ products in parental cells (Figure 4A, NHEJ branch). NHEJ products in BCR/ABL cells contained only deletions (range, −2 to −533 bp); 35% of the products lost more than 100 bp. On average, the presence of BCR/ABL induced a statistically significant ($P = .01$) loss of DNA during NHEJ.

Discussion

A mutator phenotype in cancer cells represents a major factor contributing to malignant progression of the disease.[48] In general, 2 aberrant functions may be attributed to genomic instability: enhanced DNA damage and compromised DNA repair mechanisms. DNA damage can occur as a result of the activity of endogenous compounds such as ROSs and exogenous factors such radiation or genotoxic compounds.[49] The DNA repair machinery may be deregulated by loss or gain of function.[50,51]

BCR/ABL cells treated with genotoxic agents displayed higher levels of DNA damage and aberrant DNA repair mechanisms.[5,19,20,22,52-54] These factors, combined with impaired apoptotic response and prolonged activation of the G_2/M checkpoint, can lead to genomic instability in BCR/ABL cells surviving the treatment.[4] However, we show here that even untreated BCR/ABL cells contained elevated levels of DNA lesions (including DSBs) compared with nontransformed cells. This effect—in agreement with other findings showing constitutive DNA damage in CML cells[53]—was observed not only in cell lines but also in primary cells, such as CML cells and murine bone marrow cells transformed by BCR/ABL. A recent report by Dierov et al[55] failed to detect spontaneous DNA damage shortly after tetracycline-induced BCR/ABL expression, suggesting that the effect may require a more sustained presence of BCR/ABL.

We found that elevated levels of DSBs in BCR/ABL cells, when compared with levels of their normal counterparts, resulted from ROS-dependent oxidative DNA damage. Stimulation of parental hematopoietic cell lines by a growth factor[56] or a BCR/ABL kinase[18] resulted in elevations of ROSs' levels compared with growth factor–starved parental cells. We cultured fully transformed growth factor–independent BCR/ABL cells and parental cells in the pretested optimal concentrations of IL-3 necessary to maintain continuous proliferation of the latter cells. In these conditions, ROSs were modestly (approximately 2-fold) enhanced in the former cells (data not shown). This effect may not be the sole factor contributing to the elevated oxidative damage in BCR/ABL cells. Degradation of the ROS-dependent oxidized nucleotides in the cytoplasm, their incorporation rate into DNA by polymerases, and repair efficiency of the oxidized bases incorporated into DNA may be modified in BCR/ABL cells.[57] In addition, BCR/ABL may provide necessary protection against apoptosis induced by these DNA lesions (eg, DSBs), allowing an accumulation of cells with damaged DNA.[58-60] This hypothesis is supported by our observation that elevations of ROS-induced γ-H2AX foci in parental cells treated with BSO were associated with apoptosis in some cells.

ROS can induce a variety of DNA lesions, such as oxidative base damage (eg, 8-oxoG) resulting from the incorporation of the oxidatively modified nucleotides (eg, 8-oxoGTP) into DNA by polymerases.[61] If not repaired properly, these lesions may lead to mutations, topoisomerase I–oxidized DNA cleavage complexes, DSBs at replication forks, and chromosome breaks detected on metaphase spreads.[15,16,62,63] Usually, oxidized bases are repaired by base excision repair, which requires the activity of a DNA glycosylase and an AP endonuclease to generate gaps in single-stranded DNA.[64] Such interruptions, if encountered by a replication fork, can cause DSBs,[62] which can be detected experimentally as γ-H2AX foci.[65] We hypothesize that ROS-mediated oxidative DNA lesions in BCR/ABL cells produce numerous DNA repair intermediates, which do not induce the G_1/S checkpoint in BCR/ABL cells,[5,66] resulting in DSBs at the replication forks. This speculation is supported by the finding that BCR/ABL cells containing numerous γ-H2AX foci (marker of DSBs) were detected almost exclusively in S and G_2/M phase, but not in G_0/G_1 phase. This is in agreement with the previous observation that G_1 cell cycle phase arrest prevented ROS-induced DNA strand breaks.[67] We were able to detect a few cells with γ-H2AX foci in G_1 phase, in agreement with a report that ROS caused DSBs in serum-starved G_1-phase fibroblasts.[68]

We suggest that ROS-dependent DSBs present in BCR/ABL cells occurred in the regions containing multiple 5- to 9-bp stretches of G/C. This supports findings that oxidative damage is predominantly detected in G/C-rich sequences.[69] Thus, it is intriguing to speculate that attempts to repair extensive clustered oxidative damage in BCR/ABL cells may generate DNA lesions that pose a serious obstacle for replication forks and result in DSBs. Lower levels of ROSs in normal cells may cause limited DNA damage, resulting in fewer DSBs, as suggested by the detection of fewer γ-H2AX foci. Interestingly, LL-PCR did not detect DSBs in parental cells, which may simply reflect the limited sensitivity of the assay or the formation of γ-H2AX foci on the lesions that are different from those of DSBs. γ-H2AX foci may also be detected on single-stranded DNA at arrested replication forks.[70] We speculate that less abundant oxidative damage in parental and PDTC-treated BCR/ABL cells may cause stalling of a replication fork, which could be resolved by fork regression followed by reverse branch migration, without generation of a DSB. On the other hand, extensive oxidative DNA damage in BCR/ABL-positive cells may poise the mechanisms of fork regression/resetting, more frequently resulting in DSBs. Suggested defects in the activation of the intra–S-phase checkpoint in BCR/ABL cells may also facilitate the generation of DSBs.[55]

BCR/ABL cells have to develop protective mechanisms in response to ROS-dependent chronic genotoxic stress causing DSBs (eg, prevention of caspase-3 activation and stimulation of DSB repair).[4] HRR and NHEJ represent 2 major mechanisms of DSB repair.[71] We show here that most ROS-mediated DSBs occur in S and G_2/M cell cycle phases, when both mechanisms are active and are competing for a DSB substrate.[42-44] This work supports previous findings that BCR/ABL stimulates HRR[20] and NHEJ[52,53] reactions. Moreover, RAD51 and Ku70 colocalize with γ-H2AX

foci (DSB marker) with the same relative frequency, suggesting that HRR and NHEJ have an equal opportunity to be used. Genetic analysis of the DSB repair products supports this hypothesis; approximately 40% and 60% of these products were repaired by HRR and NHEJ, respectively. The modest shift toward NHEJ frequency, in comparison with that suggested by colocalization studies, may be explained by the observation that repair of some DSBs may be initiated by homologous invasion and completed by an NHEJ mechanism.[72] In summary, we hypothesize that HRR and NHEJ play important roles in the repair of ROS-mediated DBSs in BCR/ABL cells.

We show that though they are enhanced, DSB repair mechanisms are not faithful in BCR/ABL cells. Mutations and large deletions were detected in HRR and NHEJ products, respectively. Because the mutations are scattered, not clustered near the DSBs induced by I-*Sce*I or those detected by LL-PCR, the mechanisms responsible for ROS-dependent DSBs may be different from those causing HRR-mediated mutagenesis. We hypothesize that clustered oxidative damage in G/C-rich regions may cause DSBs, whereas DNA polymerase–mediated mispairing opposite an oxidized base during HRR-dependent DNA replication may be responsible for the mutagenic effect. In addition, error-prone DNA polymerases, such as polymerase β (polβ), the expression of which is elevated in BCR/ABL cells,[9] may eventually replace other polymerases usually involved in DNA replication during HRR.[73] Interestingly, base misincorporations made during DSB repair in *Saccharomyces cerevisiae* were not substrates for the mismatch repair machinery.[74] Therefore, mismatched bases incorporated to the HRR sites might not be removed efficiently, causing mutations in the recombination products. The molecular explanation for extensive degradation of DSBs preceding NHEJ in BCR/ABL cells is unknown. Aberrantly regulated exonucleases such as ExoI, Mre11, and Artemis could be suggested as potential mediators of this reaction.[75]

CML cells accumulate genetic abnormalities during the course of the disease.[76] The most frequently observed involve additional chromosomes (Ph, +8, +19); isochromosome i(17q) associated with the loss of p53; reciprocal translocations (3;21 and 7;11) associated with the expression of AML-1/Evi-1 and NUP98/HOXA9 fusion proteins, respectively; other translocations and inversions associated with AML/myelodysplasia (inv(3), t(15;17)); loss of heterozygosity (LOH) at 14q32; homozygous mutations/deletions of pRb and p16/ARF; and mutations in p53 and RAS. The origin of these effects is mostly unknown, but errors in the repair of ROS-dependent DSBs described here can lead to the latter phenomena, especially to these involving intrachromosomal deletions and point mutations. Therefore, we hypothesize that genetic instability leading to the malignant progression of Ph-positive leukemias is associated with unfaithful repair of ROS-mediated DSBs.

In addition to BCR/ABL, myeloid cells transformed with other forms of the oncogenic ABL kinase, TEL/ABL and v-ABL, display the symptoms of ROS-dependent genotoxic stress (data not shown). Thus, unfaithful repair of ROS-dependent DSBs may represent a more universal mechanism of gaining a mutator phenotype in tumors caused by the ABL kinases and possibly also in those expressing other fusion tyrosine kinases (FTKs; BCR/FGFR, TEL/ABL, TEL/JAK2, TEL/PDGFβR, NPM/ALK).[77] Moreover, a recent report by Heath and Cross[78] shows that hematopoietic cells transformed by another FTK, ZNF198/FGFR1, which is associated with a disease that closely resembles BCR/ABL-positive CML, stimulate signal transducer and activator of transcription 5 (STAT5) to induce RAD51 and Bcl-xL expression, in accordance with our finding regarding other FTKs.[5] Thus, cells transformed by FTKs seem to be prepared to handle increased levels of ROS-dependent DSBs.

References

1. Epner DE, Koeffler HP. Molecular genetic advances in chronic myelogenous leukemia. Ann Intern Med. 1990;113:3-6.
2. Clark SS, McLaughlin J, Timmons M, et al. Expression of a distinctive BCR-ABL oncogene in Ph1-positive acute lymphocytic leukemia (ALL). Science. 1988;239:775-777.
3. Sawyers CL. Signal transduction pathways involved in BCR-ABL transformation. Baillieres Clin Haematol. 1997;10:223-231.
4. Skorski T. BCR/ABL regulates response to DNA damage: the role in resistance to genotoxic treatment and in genomic instability. Oncogene. 2002; 21:8591-8604.
5. Slupianek A, Hoser G, Majsterek I, et al. Fusion tyrosine kinases induce drug resistance by stimulation of homology-dependent recombination repair, prolongation of G(2)/M phase, and protection from apoptosis. Mol Cell Biol. 2002;22:4189-4201.
6. Shet AS, Jahagirdar BN, Verfaillie CM. Chronic myelogenous leukemia: mechanisms underlying disease progression. Leukemia. 2002;16:1402-1411.
7. Ilaria R Jr. Bcr/Abl, leukemogenesis, and genomic instability: a complex partnership. Leuk Res. 2002;26:971-973.
8. Salloukh HF, Laneuville P. Increase in mutant frequencies in mice expressing the BCR-ABL activated tyrosine kinase. Leukemia. 2000;14:1401-1404.
9. Canitrot Y, Lautier D, Laurent G, et al. Mutator phenotype of BCR-ABL transfected Ba/F3 cell lines and its association with enhanced expression of DNA polymerase beta. Oncogene. 1999; 18:2676-2680.
10. Canitrot Y, Falinski R, Louat T, et al. p210 BCR/ABL kinase regulates nucleotide excision repair (NER) and resistance to ultraviolet (UV) radiation. Blood. 2003;102:2632-2637.
11. Klucher KM, Lopez DV, Daley GQ. Secondary mutation maintains the transformed state in BaF3 cells with inducible BCR/ABL expression. Blood. 1998;91:3927-3934.
12. Deutsch E, Jarrousse S, Buet D, et al. Down-regulation of BRCA1 in BCR-ABL–expressing hematopoietic cells. Blood. 2003;101:4583-4588.
13. Cadenas E, Davies KJ. Mitochondrial free radical generation, oxidative stress, and aging. Free Radic Biol Med. 2000;29:222-230.
14. Henle ES, Linn S. Formation, prevention, and repair of DNA damage by iron/hydrogen peroxide. J Biol Chem. 1997;272:19095-19098.
15. Wang D, Kreutzer DA, Essigmann JM. Mutagenicity and repair of oxidative DNA damage: insights from studies using defined lesions. Mutat Res. 1998;400:99-115.
16. Karanjawala ZE, Murphy N, Hinton DR, Hsieh CL, Lieber MR. Oxygen metabolism causes chromosome breaks and is associated with the neuronal apoptosis observed in DNA double-strand break repair mutants. Curr Biol. 2002;12: 397-402.
17. Loft S, Poulsen HE. Cancer risk and oxidative DNA damage in man. J Mol Med. 1996;74:297-312.
18. Sattler M, Verma S, Shrikhande G, et al. The BCR/ABL tyrosine kinase induces production of reactive oxygen species in hematopoietic cells. J Biol Chem. 2000;275:24273-24278.
19. Deutsch E, Dugray A, AbdulKarim B, et al. BCR-ABL down-regulates the DNA repair protein DNA-PKcs. Blood. 2001;97:2084-2090.
20. Slupianek A, Schmutte C, Tombline G, et al. BCR/ABL regulates mammalian RecA homologs, resulting in drug resistance. Mol Cell. 2001;8:795-806.
21. Maru Y, Bergmann E, Coin F, Egly JM, Shibuya M. TFIIH functions are altered by the P210BCR-ABL oncoprotein produced on the Philadelphia chromosome. Mutat Res. 2001;483:83-88.
22. Laurent E, Mitchell DL, Estrov Z, et al. Impact of p210(Bcr-Abl) on ultraviolet C wavelength-induced DNA damage and repair. Clin Cancer Res. 2003;9:3722-3730.
23. Nowicki MO, Pawlowski P, Fischer T, Hess G, Pawlowski T, Skorski T. Chronic myelogenous leukemia molecular signature. Oncogene. 2003; 22:3952-3963.
24. Skorski T, Kanakaraj P, Nieborowska-Skorska M, et al. Phosphatidylinositol-3 kinase activity is regulated by BCR/ABL and is required for the growth of Philadelphia chromosome-positive cells. Blood. 1995;86:726-736
25. Pierce AJ, Johnson RD, Thompson LH, Jasin M. XRCC3 promotes homology-directed repair of DNA damage in mammalian cells. Genes Dev. 1999;13:2633-2638.
26. Singh NP, McCoy MT, Tice RR, Schneider EL. A simple technique for quantitation of low levels of DNA damage in individual cells. Exp Cell Res. 1988;175:184-191.

27. Majsterek I, Blasiak J, Mlynarski W, Hoser G, Skorski T. Does the bcr/abl-mediated increase in the efficacy of DNA repair play a role in the drug resistance of cancer cells? Cell Biol Int. 2002;26: 363-370.
28. Tice RR, Agurell E, Anderson D, et al. Single cell gel/comet assay: guidelines for in vitro and in vivo genetic toxicology testing. Environ Mol Mutagen. 2000;35:206-221.
29. Blasiak J, Gloc E, Wozniak K, et al. Genotoxicity of idarubicin and its modulation by vitamins C and E and amifostine. Chem Biol Interact. 2002;140: 1-18.
30. Baumann P, West SC. DNA end-joining catalyzed by human cell-free extracts. Proc Natl Acad Sci U S A. 1998;95:14066-14070.
31. Trojanek J, Ho T, Del Valle L, et al. Role of the insulin-like growth factor I/insulin receptor substrate 1 axis in Rad51 trafficking and DNA repair by homologous recombination. Mol Cell Biol. 2003;23:7510-7524.
32. Pierce AJ, Hu P, Han M, Ellis N, Jasin M. Ku DNA end-binding protein modulates homologous repair of double-strand breaks in mammalian cells. Genes Dev. 2001;15:3237-3242.
33. Schlissel M, Constantinescu A, Morrow T, Baxter M, Peng A. Double-strand signal sequence breaks in V(D)J recombination are blunt, 5′-phosphorylated, RAG-dependent, and cell cycle regulated. Genes Dev. 1993;7:2520-2532.
34. Druker BJ, Tamura S, Buchdunger E, et al. Effects of a selective inhibitor of the Abl tyrosine kinase on the growth of Bcr-Abl positive cells. Nat Med. 1996;2:561-566
35. Young HK, Floyd RA, Maidt ML, Dynlacht JR. Evaluation of nitrone spin-trapping agents as radioprotectors. Radiat Res. 1996;146:227-231.
36. Rogakou EP, Boon C, Redon C, Bonner WM. Megabase chromatin domains involved in DNA double-strand breaks in vivo. J Cell Biol. 1999; 146:905-916.
37. Burma S, Chen BP, Murphy M, Kurimasa A, Chen DJ. ATM phosphorylates histone H2AX in response to DNA double-strand breaks. J Biol Chem. 2001;276:42462-42467.
38. Ward IM, Chen J. Histone H2AX is phosphorylated in an ATR-dependent manner in response to replicational stress. J Biol Chem. 2001;276: 47759-47762.
39. Ames BN, Shigenaga MK, Hagen TM. Oxidants, antioxidants, and the degenerative diseases of aging. Proc Natl Acad Sci U S A. 1993;90:7915-7922.
40. Zhou BB, Anderson HJ, Roberge M. Targeting DNA checkpoint kinases in cancer therapy. Cancer Biol Ther. 2003;2:S16-S22.
41. Capizzi RL, Jameson JW. A table for the estimation of the spontaneous mutation rate of cells in culture. Mutat Res. 1973;17:147-148.
42. Allen C, Halbrook J, Nickoloff JA. Interactive competition between homologous recombination and non-homologous end joining. Mol Cancer Res. 2003;1:913-920.
43. Rothkamm K, Kruger I, Thompson LH, Lobrich M. Pathways of DNA double-strand break repair during the mammalian cell cycle. Mol Cell Biol. 2003; 23:5706-5715.
44. Lundin C, Erixon K, Arnaudeau C, et al. Different roles for nonhomologous end joining and homologous recombination following replication arrest in mammalian cells. Mol Cell Biol. 2002;22:5869-5878.
45. Labhart P. Nonhomologous DNA end joining in cell-free systems. Eur J Biochem. 1999;265:849-861.
46. Paull TT, Rogakou EP, Yamazaki V, Kirchgessner CU, Gellert M, Bonner WM. A critical role for histone H2AX in recruitment of repair factors to nuclear foci after DNA damage. Curr Biol. 2000; 10:886-895.
47. Meister A. Selective modification of glutathione metabolism. Science. 1983;220:472-477.
48. Loeb LA. A mutator phenotype in cancer. Cancer Res. 2001;61:3230-3239.
49. Jackson AL, Newcomb TG, Loeb LA. Origin of multiple mutations in human cancers. Drug Metab Rev. 1998;30:285-304.
50. Bishop AJ, Schiestl RH. Homologous recombination as a mechanism of carcinogenesis. Biochim Biophys Acta. 2001;1471:M109-M121.
51. Fishel R. Signaling mismatch repair in cancer. Nat Med. 1999;5:1239-1241.
52. Gaymes TJ, Mufti GJ, Rassool FV. Myeloid leukemias have increased activity of the nonhomologous end-joining pathway and concomitant DNA misrepair that is dependent on the Ku70/86 heterodimer. Cancer Res. 2002;62:2791-2797.
53. Brady N, Gaymes TJ, Cheung M, Mufti GJ, Rassool FV. Increased error-prone NHEJ activity in myeloid leukemias is associated with DNA damage at sites that recruit key nonhomologous end-joining proteins. Cancer Res. 2003;63:1798-1805.
54. Hoser G, Majsterek I, Romana DL, Slupianek A, Blasiak J, Skorski T. Fusion oncogenic tyrosine kinases alter DNA damage and repair after genotoxic treatment: role in drug resistance? Leuk Res. 2003;27:267-273.
55. Dierov J, Dierova R, Carroll M. BCR/ABL translocates to the nucleus and disrupts an ATR-dependent intra-S phase checkpoint. Cancer Cell. 2004;5:275-285.
56. Sattler M, Winkler T, Verma S, et al. Hematopoietic growth factors signal through the formation of reactive oxygen species. Blood. 1999;93:2928-2935.
57. Sekiguchi M, Tsuzuki T. Oxidative nucleotide damage: consequences and prevention. Oncogene. 2002;21:8895-8904.
58. Amarante-Mendes GP, McGahon AJ, Nishioka WK, Afar DE, Witte ON, Green DR. Bcl-2-independent Bcr-Abl-mediated resistance to apoptosis: protection is correlated with up regulation of Bcl-xL. Oncogene. 1998;16:1383-1390.
59. Amarante-Mendes GP, Naekyung Kim C, Liu L, et al. Bcr-Abl exerts its antiapoptotic effect against diverse apoptotic stimuli through blockage of mitochondrial release of cytochrome C and activation of caspase-3. Blood. 1998;91:1700-1705.
60. Dubrez L, Eymin B, Sordet O, Droin N, Turhan AG, Solary E. BCR-ABL delays apoptosis upstream of procaspase-3 activation. Blood. 1998; 91:2415-2422.
61. Jackson AL, Loeb LA. The contribution of endogenous sources of DNA damage to the multiple mutations in cancer. Mutat Res. 2001;477:7-21.
62. Kuzminov A. Single-strand interruptions in replicating chromosomes cause double-strand breaks. Proc Natl Acad Sci U S A. 2001;98:8241-8246.
63. Daroui P, Desai SD, Li TK, Liu AA, Liu LF. Hydrogen peroxide induces topoisomerase I-mediated DNA damage and cell death. J Biol Chem. 2004; 279:14587-14594.
64. Lu AL, Li X, Gu Y, Wright PM, Chang DY. Repair of oxidative DNA damage: mechanisms and functions. Cell Biochem Biophys. 2001;35:141-170.
65. Limoli CL, Giedzinski E, Bonner WM, Cleaver JE. UV-induced replication arrest in the xeroderma pigmentosum variant leads to DNA double-strand breaks, gamma -H2AX formation, and Mre11 relocalization. Proc Natl Acad Sci U S A. 2002;99: 233-238.
66. Nishii K, Kabarowski JH, Gibbons DL, et al. ts BCR-ABL kinase activation confers increased resistance to genotoxic damage via cell cycle block. Oncogene. 1996;13:2225-2234.
67. Rancourt RC, Hayes DD, Chess PR, Keng PC, O'Reilly MA. Growth arrest in G1 protects against oxygen-induced DNA damage and cell death. J Cell Physiol. 2002;193:26-36.
68. Vafa O, Wade M, Kern S, et al. c-Myc can induce DNA damage, increase reactive oxygen species, and mitigate p53 function: a mechanism for oncogene-induced genetic instability. Mol Cell. 2002;9: 1031-1044.
69. Akman SA, O'Connor TR, Rodriguez H. Mapping oxidative DNA damage and mechanisms of repair. Ann N Y Acad Sci. 2000;899:88-102.
70. Ward IM, Minn K, Chen J. UV-induced ATR activation requires replication stress. J Biol Chem. 2004;279:9677-9680.
71. Khanna KK, Jackson SP. DNA double-strand breaks: signaling, repair and the cancer connection. Nat Genet. 2001;27:247-254.
72. Richardson C, Jasin M. Coupled homologous and nonhomologous repair of a double-strand break preserves genomic integrity in mammalian cells. Mol Cell Biol. 2000;20:9068-9075.
73. Servant L, Bieth A, Hayakawa H, Cazaux C, Hoffmann JS. Involvement of DNA polymerase beta in DNA replication and mutagenic consequences. J Mol Biol. 2002;315:1039-1047.
74. McGill CB, Holbeck SL, Strathern JN. The chromosome bias of misincorporations during double-strand break repair is not altered in mismatch repair-defective strains of *Saccharomyces cerevisiae*. Genetics. 1998;148:1525-1533.
75. Lieber MR, Ma Y, Pannicke U, Schwarz K. Mechanism and regulation of human non-homologous DNA end-joining. Nat Rev Mol Cell Biol. 2003;4:712-720.
76. Calabretta B, Perrotti D. The biology of CML blast crisis. Blood. 2004;103:4010-4022.
77. Skorski T. Oncogenic tyrosine kinases and the DNA-damage response. Nat Rev Cancer. 2002;2: 351-360.
78. Heath C, Cross NC. Critical role of STAT5 activation in transformation mediated by ZNF198-FGFR1. J Biol Chem. 2004;279:6666-6673.